J. metamorphic Geol., 2009, **27,** 423–437 doi:10.1111/j.1525-1314.2009.00824.x

Microstructural, chemical and textural records during growth of snowball garnet

M. ROBYR,[1]* W. D. CARLSON,[1] C. PASSCHIER[2] AND P. VONLANTHEN[3]
[1]*Department of Geological Sciences, University of Texas, Austin, 78731 Texas, USA (martin.robyr@geo.unibe.ch)*
[2]*Department of Geosciences, University of Mainz, 55099 Mainz, Germany*
[3]*Institute of Geology and Palaeontology, University of Lausanne, CH-1015 Lausanne, Switzerland*

ABSTRACT The growth history of two populations of snowball garnet from the Lukmanier Pass area (central Swiss Alps) was examined through a detailed analysis of three-dimensional geometry, chemical zoning and crystallographic orientation. The first population, collected in the hinge of a chevron-type fold, shows an apparent rotation of 360°. The first 270° are characterized by spiral-shaped inclusion trails, gradual and concentric Mn zoning and a single crystallographic orientation, whereas in the last 90°, crenulated inclusion trails and secondary Mn maxima centred on distinct crystallographic garnet domains are observed. Microstructural, geochemical and textural data indicate a radical change in growth regime between the two growth sequences. In the first 270°, growth occurred under rotational non-coaxial flow, whereas in the last 90°, garnet grew under a non-rotational shortening regime. The second population, collected in the limb of the same chevron-type fold structure, is characterized by a spiral geometry that does not exceed 270° of apparent rotation. These garnet microstructures do not record any evidence for a modification of the stress field during garnet growth. Concentric Mn zoning as well as a single crystallographic orientation are observed for the entire spiral. Electron backscatter diffraction data indicate that nearly all central domains in the snowball garnet are characterized by one [001] axis oriented (sub-)parallel to the symmetry axis and by another [001] axis oriented (sub-)parallel to the orientation of the internal foliation. These features suggest that the crystallographic orientation across the garnet spiral is not random and that a relation exists among the symmetry axis, the internal foliation and the crystallographic orientation.

Key words: electron backscatter diffraction; lukmanier; snowball garnet; tomography.

INTRODUCTION

One challenge for geologists is to interpret correctly the mineral textures and microstructures resulting from orogenic processes. The progressive response of rocks to the modification of pressure, temperature and stress-field conditions associated with large-scale tectonic processes within the crust leads to the formation of specific fabrics that can be used to reconstruct the tectono-metamorphic history of rocks. Garnet porphyroblasts provide key information on the evolution of geological terranes, mainly because of their ability to record the modifications of external conditions and to preserve microstructures and detailed compositional zoning over a wide range of metamorphic grades.

The timing of mineral growth and deformation can be deciphered based on the geometrical relation between inclusion trails and matrix fabric. Sigmoidal and spiral-shaped inclusion trails, like those observed in snowball garnet, are traditionally interpreted as evidence for syn-kinematic porphyroblast growth (Spry, 1963; Rosenfeld, 1970; Schoneveld, 1977). Snowball garnet is therefore considered as an explicit shear-sense indicator and has been used extensively to interpret the tectono-metamorphic history of rocks. In spite of this, however, the mechanisms responsible for their formation remain unclear and two models have been put forward over the last two decades. The first model (Fig. 1a) argues for porphyroblast rotation with respect to the foliation in a single tectonic phase of non-coaxial flow (Spry, 1963; Rosenfeld, 1970; Schoneveld, 1977; Passchier *et al*., 1992; Gray & Busa, 1994; Williams & Jiang, 1999; Ikeda *et al*., 2002). In this interpretation, the growth of snowball garnet is explained by continuous and synchronous porphyroblast rotation in response to shear at a small angle with respect to the external foliation.

A second model, first suggested by Ramsay (1962), holds that under conditions of coaxial, non-rotational flow, rigid porphyroblasts may remain spatially fixed during deformation while the matrix fabric is rotating around them. Mancktelow *et al*. (2002) showed that even in non-coaxial, rotational flow, porphyroblasts and other large objects might remain spatially fixed with respect to the foliation and the lineation if coupling between the object and the matrix is incomplete and sectored (Schmid & Podladchikov, 2004).

**Present address*: Institute of Geological Sciences, University of Bern, CH-3012 Bern, Switzerland

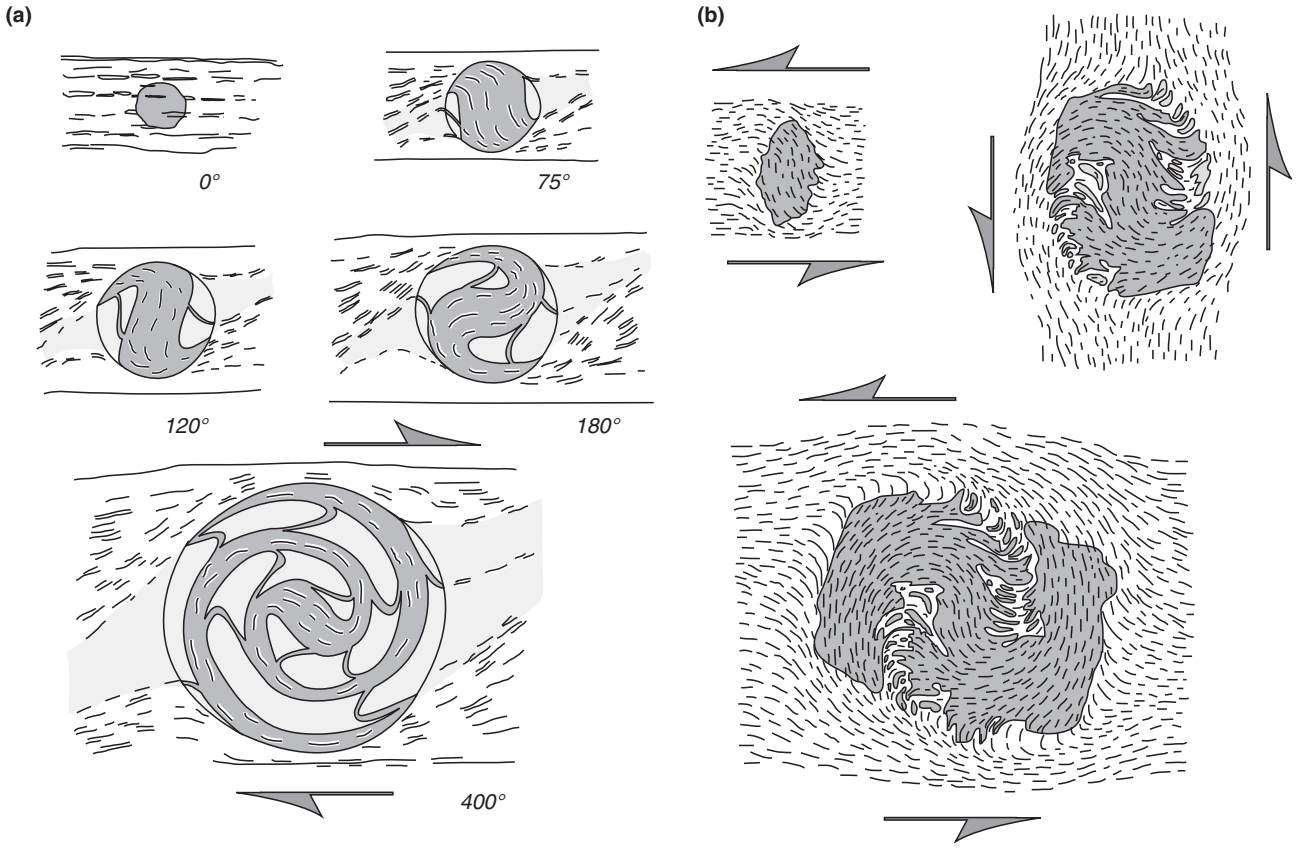

Fig. 1. Schematic view illustrating the formation of snowball garnet porphyroblasts according to the two classical end-member models. (a) Simultaneous growth and rotation model presented by Schoneveld (1977). The garnet grain rotates with respect to a stationary external foliation in dextral non-coaxial flow. (b) Strain-partitioning model proposed by Bell (1985). This model postulates the rotation of the foliation around a stationary porphyroblast in sinistral coaxial flow (modified from Johnson, 1993). The two end-member models predict a similar spiral geometry but opposite senses of shear.

Consistently with these considerations, the suggestion was made that snowball garnet results from the rotation of the foliation while garnet porphyroblasts are kept fixed, even in non-coaxial flow. In such a model (Fig. 1b), referred to as the strain-partitioning model (Bell, 1985), garnet successively overprints the new generations of near-orthogonal foliations produced by successive episodes of shortening and extension occurring during porphyroblast growth (e.g. Bell & Rubenach, 1983; Bell & Johnson, 1989; Johnson, 1990; Bell *et al*., 1992; Aerden, 1995; Johnson & Bell, 1996; Hickey & Bell, 1999; Stallard, 2003). Thus, the question of whether snowball garnet rotates or not carries particular significance in structural geology, not only because the two end-member models predict opposite shear senses, but also because they imply single *v*. polyphase deformation histories.

The contradictory interpretations that arise from the two models have led to the quest for unambiguous criteria to distinguish between rotational and non-rotational growth. However, despite passionate debates and several pairs of opposing papers published over the last two decades (Bell *et al*., 1992 and Busa & Gray, 1992; Passchier *et al*., 1992 and Visser & Mancktelow, 1992; Forde & Bell, 1993 and Johnson, 1993; Vernon *et al*., 1993 and Bell & Hickey, 1999; Hickey & Bell, 1999 and Williams & Jiang, 1999; Ikeda *et al*., 2002 and Stallard, 2003), the issue remains unresolved, mainly because neither of the two models can be ruled out solely on the basis of geometrical arguments (Johnson, 1993; Stallard *et al*., 2002). In this study, high-resolution X-ray computed tomography (HRXCT), electron-probe microanalyses (EPMA) and electron backscattered diffraction (EBSD) were used in combination with microstructural analyses and regional tectonics to bring new evidence to bear on the origin of snowball garnet porphyroblasts.

GEOLOGICAL SETTING

Snowball garnet was collected in the Lukmanier Pass area in the Central Alps, Switzerland (Fig. 2). The broad outline of the Lukmanier geology is summarized below. For a more detailed account the reader is referred to Chadwick (1968).

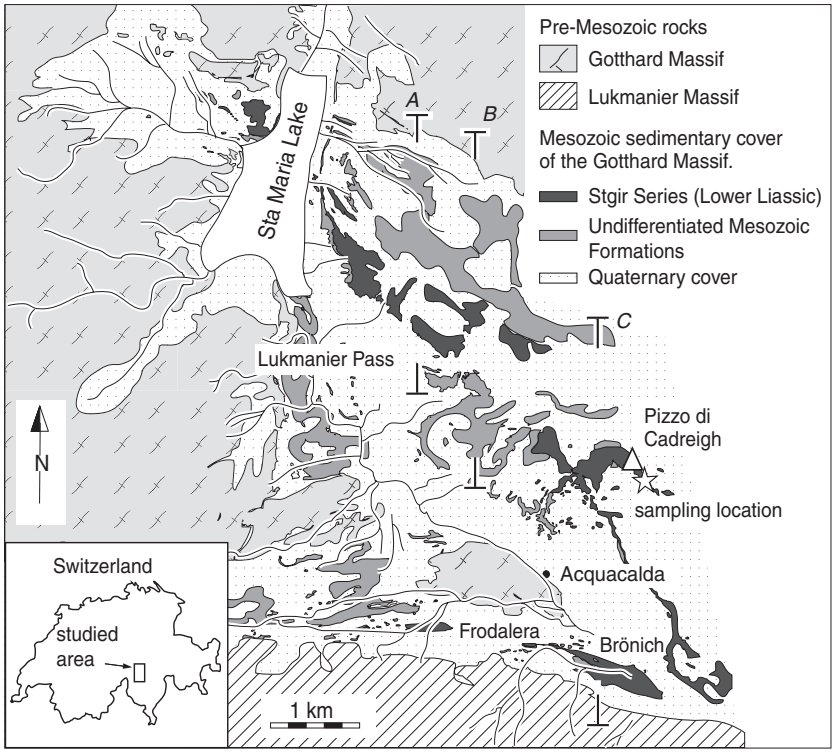

Fig. 2. Geological map of the Lukmanier Pass area in the central Swiss Alps. The sampling location for the garnet from the limb and the hinge is indicated by a triangle and a star (Swiss national grid coordinates: 707.546/156.046 and 708.163/156.045) respectively.

The Lukmanier Pass area is a natural cross-section through the northern border of the Lepontine Dome, an asymmetric metamorphic dome exposed by uplift and exhumation of the deepest part of the Alpine nappe stack (Todd & Engi, 1997). The area experienced a polyphase tectonic history with three main phases of deformation, all of them related to southward and upward tectonic movements triggered by the Tertiary continent–continent collision between the Eurasian and Apulian plates. Two major tectonic units can be distinguished: the Gotthard Massif to the north, partly overlain by Mesozoic sedimentary cover and the Lukmanier Massif to the south.

Multistage shortening structures are recorded within the Mesozoic sedimentary cover (Fig. 3). They are related to two early phases of crustal thickening (D1 & D2) associated with top-to-the-N movements, likely reflecting the southward underthrusting of the Lukmanier region beneath the frontal part of the Apulian plate. Relict D1 microstructures consist of finely spaced foliation subsequently folded into microlithons during D2. Rare F1 folds indicate that D1 was

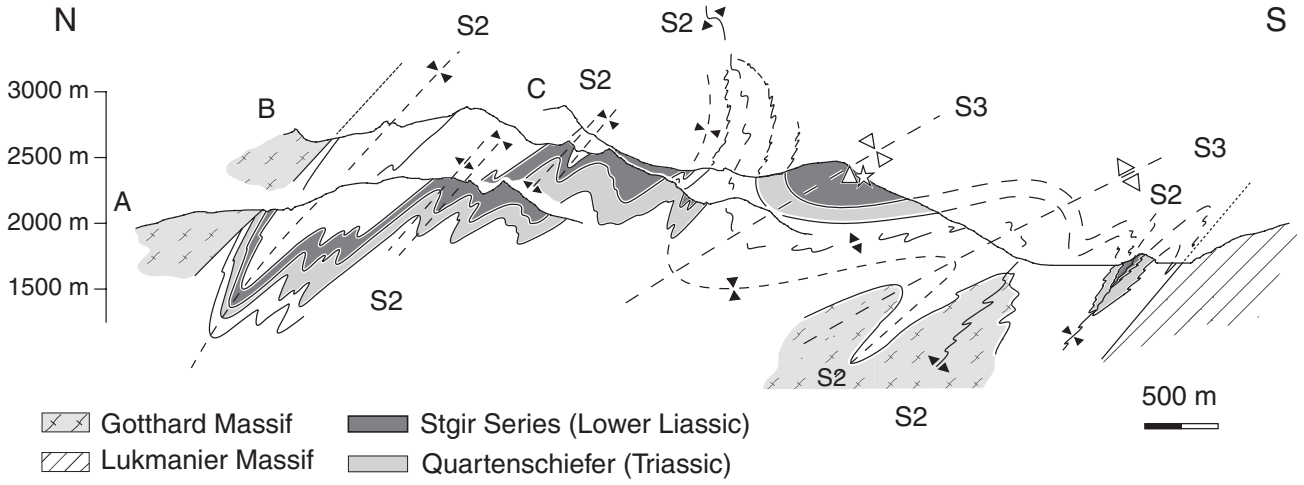

Fig. 3. Cross-section through the Lukmanier Pass area. For the location of the profiles (A), (B) and (C) see Fig. 2. Full and open arrowheads indicate synforms and antiforms related to D2 and D3 respectively.

responsible for isoclinal folding. This D1 tectonic event was responsible for imbricate stacking of basement and sedimentary cover units during Early to Middle Eocene.

A second stage of crustal thickening is expressed by D2 structures superposed on the D1 fabrics. The D2 deformation phase created the main structural elements in the Lukmanier area, such as the axial-planar surfaces of the large isoclinal folds and the main foliation (S2) which bears a penetrative, NE-plunging mineral lineation. Both S1 and S2 foliations were subsequently folded to form asymmetric, centimetre to kilometre-scale F3 folds verging to the SW. At the regional scale, the D3 folding is responsible for the overturning towards the SW of the initially NE-verging F2 folds. D3 was also accompanied by intensive SE-directed backfolding and backthrusting that led to the upward tectonic movement of crustal material and the exhumation of the Lukmanier metamorphic rocks.

Regional mapping of the mineral distributions throughout the Lukmanier Pass reveals a metamorphic field gradient characterized by peak conditions increasing gradually from the chloritoid zone north of the Santa Maria Lake, to the staurolite–kyanite zone in the Brönich area to the south (Fox, 1975). Thermobarometric analyses of metapelites indicate peak conditions evolving from 410 °C for the chloritoid zone (Rahn *et al.*, 2002) to 575 °C at 8.8 kbar for the staurolite–kyanite zone (Janots *et al.*, 2008).

SAMPLE CHARACTERIZATION

The occurrence of snowball garnet is restricted to specific metapelitic intervals of the Liassic Stgir Formation, itself belonging to the Mesozoic sedimentary cover of the Gotthard Massif (Robyr *et al.*, 2007). These intervals are characterized by thin alternations of quartz- and phyllosilicate-rich layers. Two populations of snowball garnet were investigated. The first population was sampled in the hinge of a chevron-type F3 fold, whereas the second one was collected in the limb of the same fold structure (Fig. 4).

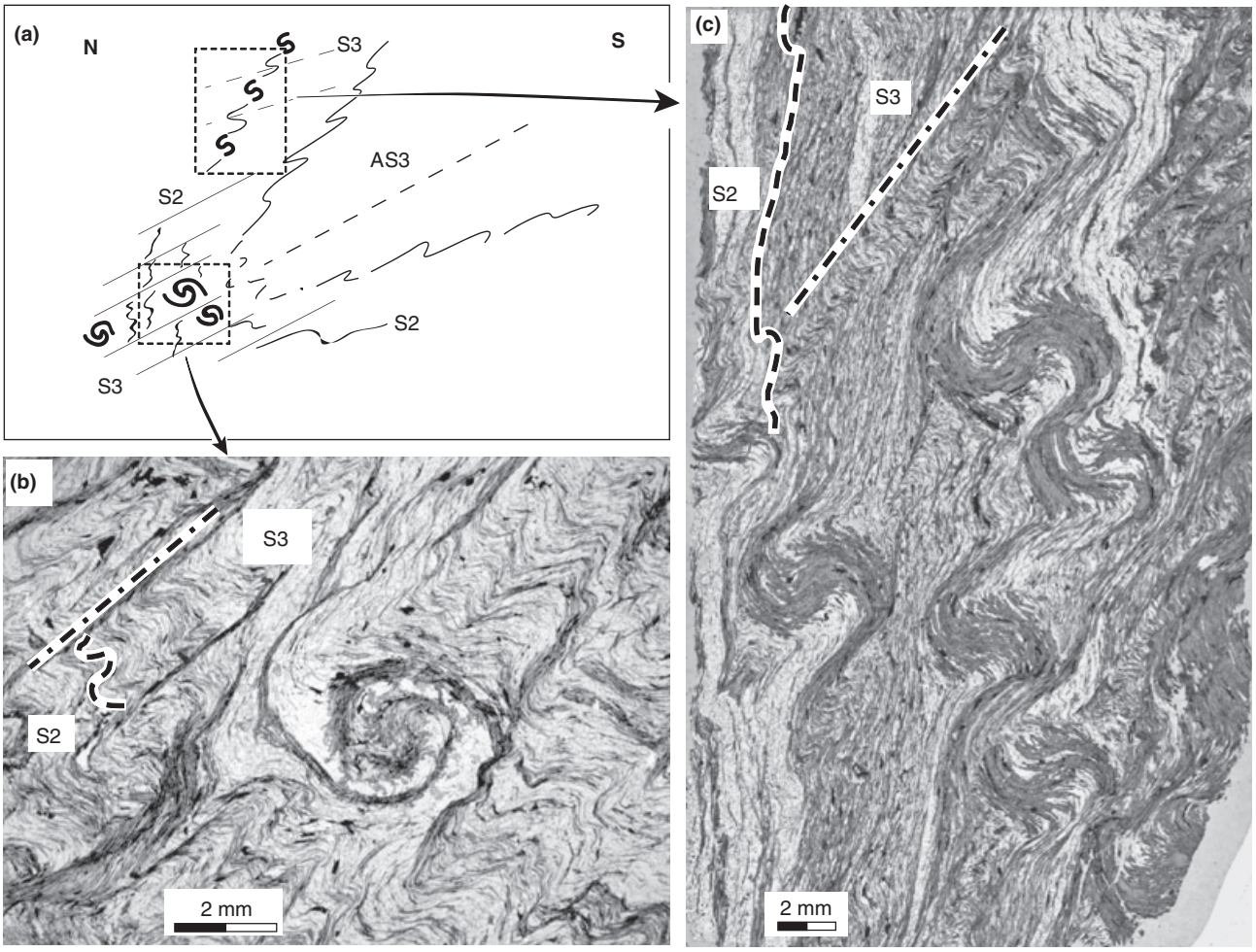

Fig. 4. (a) Synoptic sketch showing the location of the garnet porphyroblasts within the F3 fold structure; not to scale. Photomicrograph of some typical snowball garnet collected in the fold hinge (b) and in the fold limb (c).

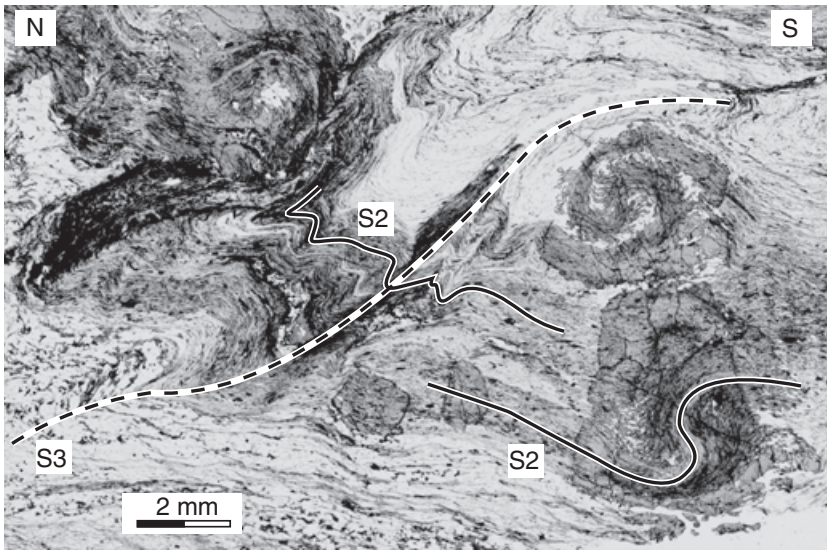

Fig. 5. Photomicrograph showing the deflection of the S3 crenulation cleavage around the snowball garnet porphyroblasts and the continuity between the spiral-shaped internal foliation and the main rock schistosity (S2).

At both sampling localities, the rocks are lithologically similar and contain the mineral assemblage garnet + muscovite + biotite + quartz + plagioclase + epidote with minor chlorite and ilmenite. The occurrence of snowball garnet exclusively within thin phyllosilicate-rich layers suggests that mica and/or chlorite were key reactants in the garnet-forming reactions.

The rock fabric is radically different in the two sampling localities. In the hinge, a NE-dipping penetrative crenulation cleavage (S3) overprints the dominant foliation (S2), resulting in the formation of closely spaced microlithons. No such cleavage is visible in the limbs. Instead, D3 deformation in the limbs resulted in the formation of secondary folds and in a weak S3. Microstructural observations show that the crenulation cleavage (S3) wraps the snowball garnet (Fig. 5), indicating that it grew mainly before D3. The continuity between the spiral-shaped internal foliation and the main rock schistosity (S2) shows that the most significant period of growth occurred during D2, even though the incorporation of the crenulated S2 foliation by garnet overgrowth clearly indicates that limited post-D2 growth has occurred as well.

Whole-rock major-element chemical data obtained by X-ray fluorescence analysis indicate that the composition of rocks in the two sampling localities is not identical (Table 1). However, the observed difference is mainly imputable to the variation in SiO_2 content between the two outcrops, which is reflected in the abundances of all the other oxides. We attribute this difference in SiO_2 content to the highly variable thickness of quartz-rich layers at the scale of the hand specimens. In order to test this interpretation, the bulk composition has been re-calculated based on an identical SiO_2 content arbitrarily fixed at 72.21 wt% in both samples (Table 2). The differences in composition after normalization are much less significant than suggested by the raw chemical data. We infer, therefore, that garnet crystallized under similar *P–T* conditions in both the hinge and the limb of the fold. This inference is also supported by the identical mineral assemblage in both outcrops.

ANALYTICAL METHODS

Three-dimensional (3D) imaging was conducted in the HRXCT facilities at the University of Lausanne (Skyscan-1072 system) and at the University of Texas at Austin (UTCT ultra-high-resolution sub-system). HRXCT was also used to identify central sections of garnet for microprobe and EBSD measurements. Chemical analyses and mapping through wavelength

Table 1. Whole-rock major-element chemistry obtained by X-ray fluorescence for the samples Luk_06_3 (fold hinge) and RM_05_6 (fold limb).

Samples	Luk_06_3	RM_05_6
SiO_2	68.87	80.21
Al_2O_3	15.01	9.23
FeO	5.69	4.17
MgO	0.87	0.53
MnO	0.06	0.02
K_2O	3.05	1.37
Na_2O	0.35	0.19
CaO	1.48	1.02
Total	95.38	96.74

Table 2. Re-calculated bulk compositions of samples from Table 1.

Samples	Luk_06_3	RM_05_6
SiO_2	72.21	72.21
Al_2O_3	15.74	15.52
FeO	5.97	7.01
MgO	0.91	0.89
MnO	0.06	0.03
K_2O	3.20	2.30
Na_2O	0.36	0.32
CaO	1.55	1.72
Total	100.00	100.00

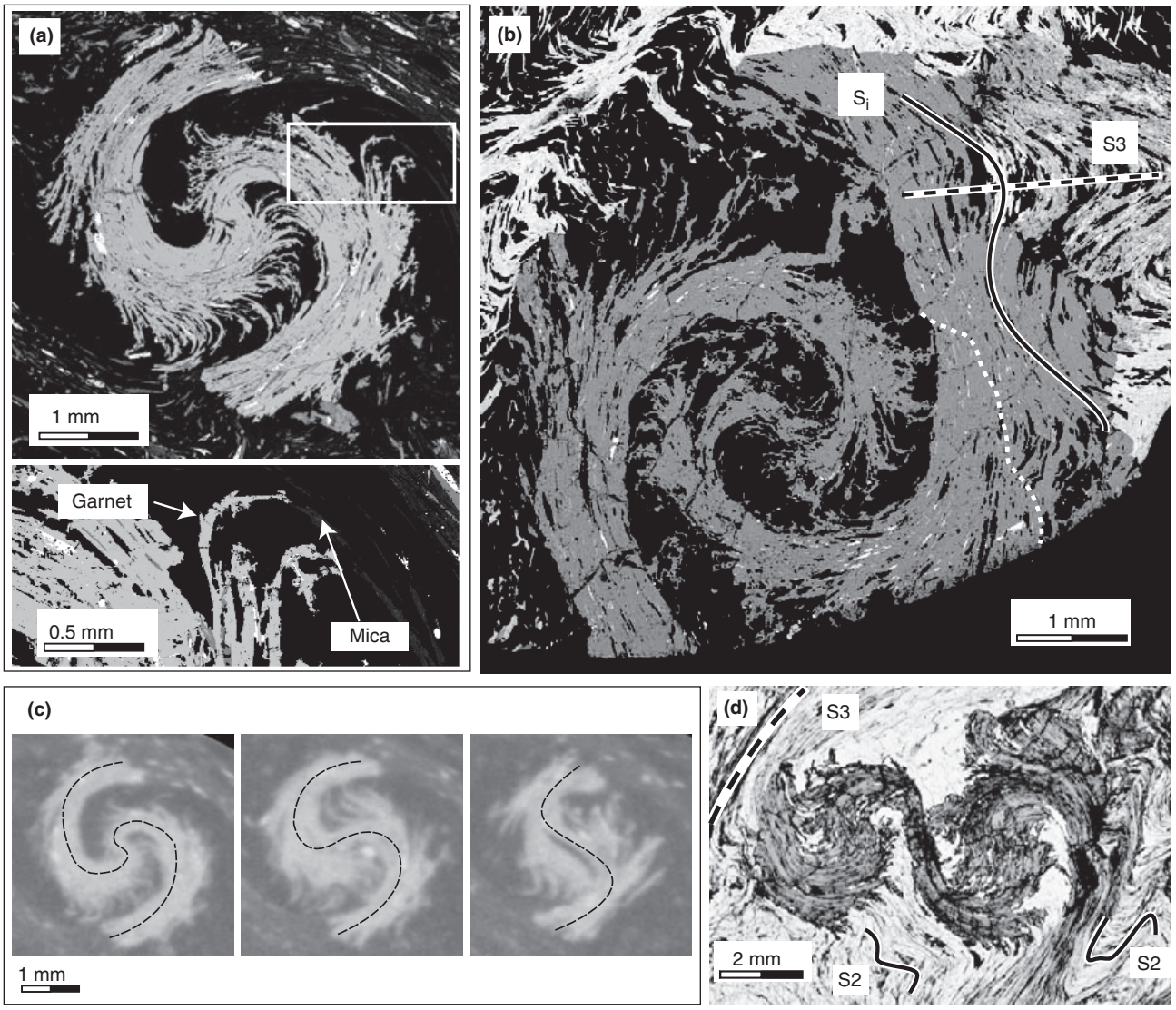

Fig. 6. Illustration of various textural characteristics observed in the snowball garnet. (a) Photomicrographs illustrating the formation of garnet bridges by replacement of mica during porphyroblast growth. (b) Al compositional map of garnet from the fold hinge showing the modification of the inclusion-trail pattern (S_i) from core to rim; the dashed line is for XMn = 0.009. (c) Selected HRXCT cross-sections perpendicular to the garnet symmetry axis illustrating the gradual decrease in spiral amplitude from the centre outwards (left to right). (d) Photomicrograph of neighbouring snowball garnet linked to each other by their arm terminations.

dispersive X-ray spectroscopy (WDS) were carried out at the University of Lausanne on a Cameca SX 50 electron microprobe and at the University of Texas on a JEOL 8200 Superprobe. Crystallographic-orientation measurements were performed by EBSD at the University of Fribourg (Switzerland) and at the University of Texas using EDAX (TSL) OIM and Oxford (HKL) Channel 5 systems mounted on FEI XL30 scanning electron microscopes.

SNOWBALL GARNET MICROSTRUCTURE AND GEOMETRY

The geometry of snowball garnet is characterized by a core region, around which two spiral arms are wound (Fig. 6). Pressure shadows of quartz gradually incorporated within the spiral volume during growth are frequently observed as relics in the matrix lying between the core and the arms of the spiral (cf. Schoneveld, 1977). The continuity of the quartz-rich domains is commonly interrupted by thin curved garnet overgrowths that bridge the core to the arms of the spiral. In a few case, however, the garnet bridges are not connected to the external arms but stop within the quartz matrix, where they connect to thin mica folia (Fig. 6a). This suggests that the bridges were originally made of mica and were replaced by garnet as the crystallization front progressed.

Within the garnet, tiny elongated oxide, epidote and graphite crystals define spiral-shaped inclusion trails.

The amount of apparent rotation recorded by inclusion trails depends systematically on the location of the snowball garnet within the F3 fold structures. Whereas the garnet collected in the fold hinge exhibits an apparent rotation of 360°, the garnet from the fold limb displays an apparent rotation that does not exceed 270° with respect to the S2 foliation (see Fig. 4).

In snowball garnet from the hinge, the geometry of the inclusion trails may change radically from spiral-shaped in the main body of the spiral to crenulated in the external rims of the spiral arms (Fig. 6b), suggesting a sudden change in the rock flow conditions. Spiral-shaped inclusion trails are often attributed to a rotational flow regime with a flow plane parallel to the foliation. In contrast, crenulation requires a shortening component normal to the foliation. In the Lukmanier Pass area, regional, non-rotational shortening during D3 has significantly crenulated the main foliation (S2) within the matrix. The perfect continuation of the crenulated foliation from the matrix through the garnet outer rims strongly suggests that the final stage of garnet growth occurred during D3. In addition, the continuity of the S3 axial surface across the garnet–matrix boundary reveals that coupling between the garnet porphyroblast and the matrix occurred during the last stage of garnet growth. This further supports the absence of rotation with respect to the external foliation at the end of garnet growth. Thus, microstructural arguments suggest that the formation of snowball garnet from the hinge occurred in a two stage process and under two different flow regimes. Whereas the first 270° of the spiral is best explained by rotation of the garnet rather than by non-rotational garnet growth over successive generations of near-orthogonal foliations, the crystallization of the last 90° of the spiral is consistent with growth under a non-rotational flow regime, in a manner that bears some similarity to the alternating deformation phases postulated in the strain-partitioning model.

In contrast, the snowball garnet collected in the limb of the F3 folds displays a more common and simple geometry than that from the fold hinge. The maximum amount of apparent rotation does not exceed 270° with respect to S2 foliation and no evidence for a modification of the stress field during garnet growth is recorded by inclusion trails. In fact, the geometry of the garnet from the fold limb is very similar to the first 270° of the garnet from the hinge, suggesting that the mechanism of growth was probably similar for both garnet populations during the first 270° of apparent rotation.

It must be noted, however, that the protracted discussion on the origin of snowball garnet has shown that it is very difficult, if not impossible, to find unequivocal evidence to differentiate between rotational and non-rotational growth. Several authors (e.g. Busa & Gray, 1992; Passchier & Trouw, 2005 and references therein), have demonstrated that microstructural observations correlated with regional tectonics and geometrical arguments are very effective for deciphering convincingly the growth mechanisms of snowball garnet. The deformation history recorded by foliations and folds in the Lukmanier Pass area, coupled with tectonic information from adjacent domains in the Alps, indicate that the tectonic phases of nappe stacking (D1) and isoclinal folding (D2) are associated with top-to-the-NNE-directed shearing (Chadwick, 1968; Thakur, 1973; Maxelon & Mancktelow, 2005). This sense of shear is corroborated by the snowball garnet if a rotational interpretation is assumed, but it is not compatible with the sense of shear expected from the strain-partitioning model. In addition, the geometry of garnet both from the limb and hinge show a gradual decrease in spiral amplitude along the symmetry axis of the spiral from the centre of the grain outwards (Fig. 6c). This pattern, which is very similar to that observed by Schoneveld (1977) by serial sectioning, is best explained by rotation of the garnet

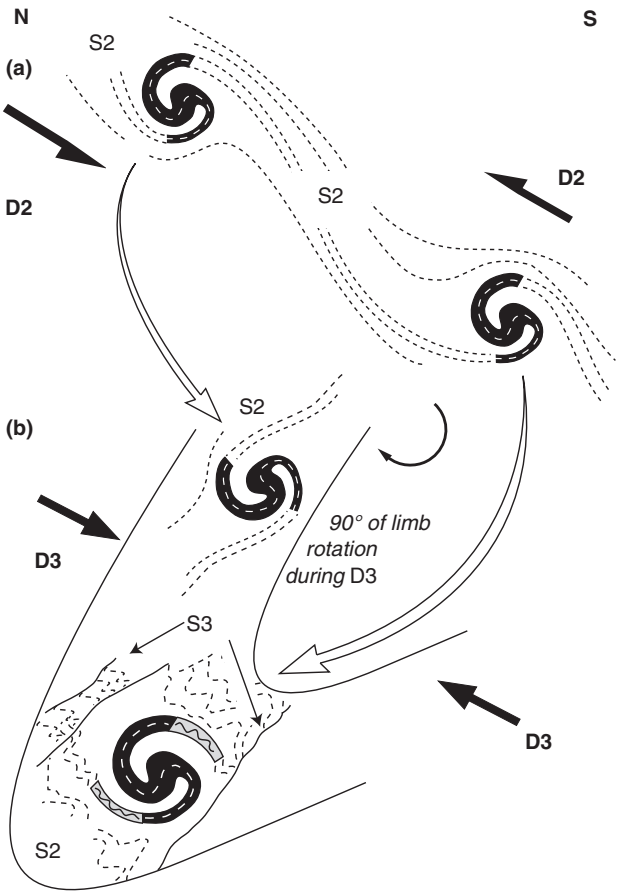

Fig. 7. Sketch model illustrating the contrasting behaviour of the snowball garnet in the fold hinge and in the fold limb, not to scale. (a) During D2, the southward underthrusting of the Lukmanier region is accompanied by simple shear: the snowball garnet grows and rotates simultaneously. (b) During D3, flexural folding leads to a cessation of growth in the garnet from the limb. In the hinge, garnet continues to grow (light grey) and overprints the S2 crenulated foliation.

during growth. Finally, rotation of the snowball garnet from the Lukmanier Pass area is also supported by the occurrence of neighbouring porphyroblasts linked to each other by their spiral terminations (Fig. 6d). If the garnet had been spatially fixed, such a configuration would require a similar rotation of the external foliation around each porphyroblast. This scenario is unlikely, considering that the presence of two contiguous garnet grains would inevitably disturb the regular rotation of the foliation.

To sum up, the geometry of the inclusion trails preserved in the core region of snowball garnet from the fold hinge and in the entire spiral structure in the garnet from the fold limb, the distribution and 3D morphology along the symmetry axis as well as the sense of shear indicated by the snowball garnet are more consistently explained by a single and continuous rotation of the crystals rather than by an incremental superimposition of foliations resulting from numerous changes in the stress field. However, textural evidence also indicates that a different, non-rotational, flow regime occurred during the last stage of crystallization of the garnet from the fold hinge (Fig. 7). These data suggest that the two previously proposed end-member models can operate successively during garnet growth.

COMPOSITIONAL ZONING

Compositional zoning in garnet has long been used as a marker reflecting the incorporation of different chemical elements through time during growth (Hollister, 1966; Kretz, 1973, 1974, 1993; Carlson, 1989, 1991; Carlson & Denison, 1992; Spear, 1993; Carlson *et al.*, 1995; Chernoff & Carlson, 1997, 1999; Denison *et al.*, 1997; Spear & Daniel, 1998; Daniel & Spear, 1999; Hirsch *et al.*, 2003; Meth & Carlson, 2005). Assuming local chemical equilibrium on the garnet–matrix boundary and no post-growth intra-crystalline diffusion, all points of the crystal belonging to the same growth interval share the same chemical composition. Thus, a variation of the chemical composition from the core to the rim of the garnet reflects successive periods of growth during garnet crystallization. In garnet from pelitic schists, the gradual decrease in Mn concentration from core to rim is therefore interpreted as an indicator of the sequestration of Mn into garnet and a corresponding depletion of Mn in the matrix.

X-ray compositional maps collected in samples from both the hinge and the limb (Fig. 8a) reveal broadly concentric zoning of most major elements, with a typical Mn and Ca enrichment in the core region. The

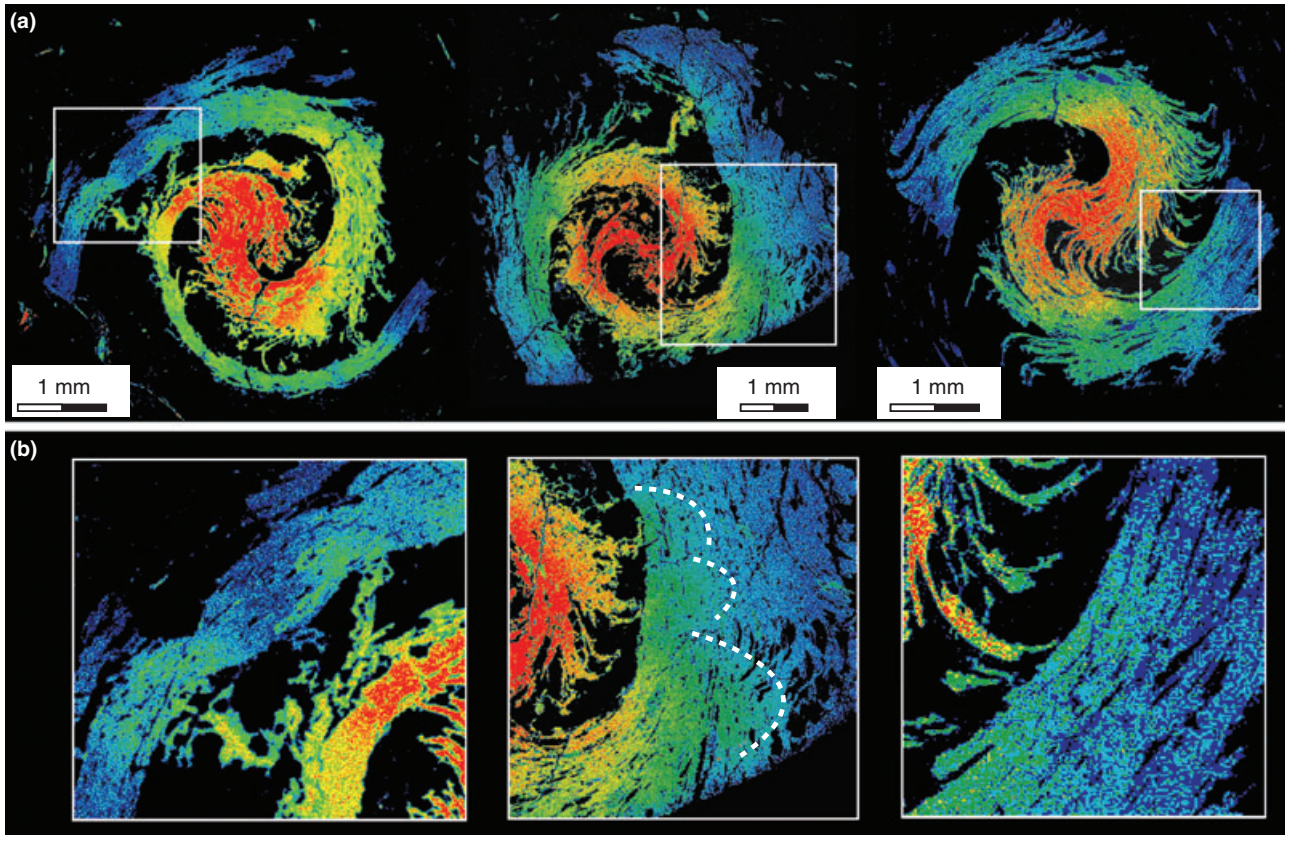

Fig. 8. (a) WDS X-ray maps of Mn for garnet collected in the hinge (left and centre) and in the limb (right). Warmer colours indicate higher concentration levels. (b) Close-up view of the framed areas in (a) showing the secondary Mn maxima and anomalously high Mn concentration across the garnet bridges.

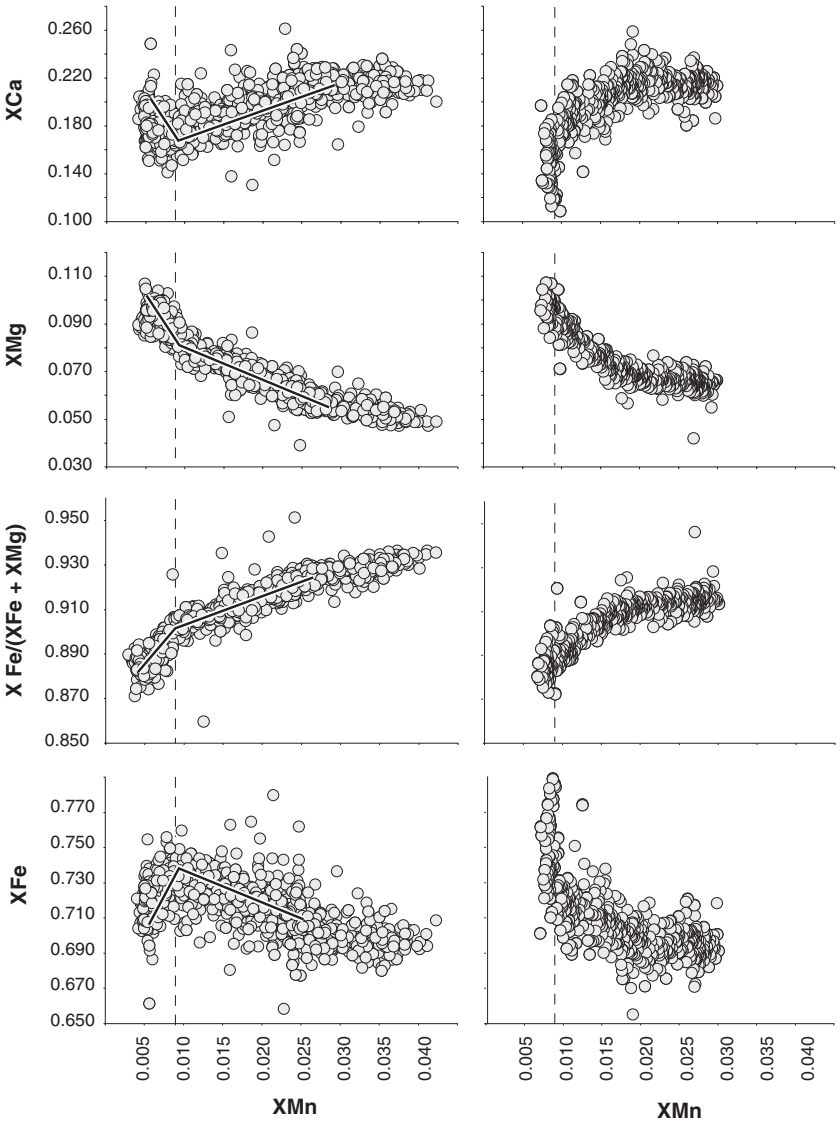

Fig. 9. Chemical diagrams based on 1421 EPMA measurements illustrating the strong correlation between the divalent cations Mn, Mg, Fe and Ca in garnet from the hinge (left) and the limb (right). XMn = 0.009 is highlighted by a dashed line.

gradual decrease in Mn and Ca concentration levels towards the rim is counterbalanced by an equivalent increase in Fe and Mg. In some garnet from the hinge, however, the regular concentric zoning pattern is commonly disturbed by anomalously high Mn concentration across garnet bridges, suggesting that the bridges served as shortcuts making the crystallization path from the core to the external arms significantly shorter (Robyr *et al*., 2007). This is further illustrated by the systematic cauliflower shapes of the Mn concentration contours at the outermost edges of the bridges (Fig. 8b), indicating that a significant portion of the garnet growth was actually controlled by crystallization along the bridges rather than through the standard crystallization path along the spiral curvature. In addition to the anomalously high Mn concentration across garnet bridges, secondary Mn maxima were also identified in the arms of the spirals (Robyr *et al*., 2007).

Chemical compositions inferred from 1421 measurements on garnet from the fold hinge and from the fold limb reveal strong correlations among the major divalent cations (Fig. 9). These correlations indicate that Mn, Mg, Fe and Ca have achieved mutual chemical equilibrium during crystallization, and they validate the use of Mn concentrations as time lines reflecting the successive crystallization stages of garnet growth. Garnet from the fold hinge has a mean core composition of XFe = 0.70, XMg = 0.05, XMn = 0.04 and XCa = 0.21 and a mean rim composition of XFe = 0.71, XMg = 0.09, XMn = 0.004 and XCa = 0.19. In garnet from the fold limb, the mean core composition is XFe = 0.69, XMg = 0.07, XMn = 0.03 and XCa = 0.21, whereas the mean rim composition is XFe = 0.74, XMg = 0.10, XMn = 0.008 and XCa = 0.15. The reason for the slightly higher Mn concentrations in the centre of the garnet from the hinge (XMn = 0.04) with respect to those from the limb

(XMn = 0.03) is not entirely clear, but the explanation may lie in small differences in whole-rock composition. The higher MnO content observed in the bulk composition of the sample from the hinge might have stabilized garnet slightly earlier during the tectonometamorphic history of the rock. Another explanation may be that the thin section may not have intersected the nucleation site of the crystal. This is supported by observations in other crystals, in which an offset of 0.5 mm from the nucleation site would have resulted in a decrease of 0.01 in the XMn value.

Compositional XMn diagrams for garnet from the fold hinge (Fig. 9) display a systematic break at XMn = 0.009, i.e. shortly before the end of crystallization at XMn = 0.004. The break is characterized by an increase in Ca concentration and an equivalent decrease in Fe and Mg. In the fold limb, the garnet does not record XMn concentration values below 0.008, suggesting that the very last stage of growth occurred at this concentration level. Contrary to what is observed in the garnet of the hinge, an abrupt decrease in Ca concentration correlated with a sharp increase in Fe and Mg is observed at the rims of the garnet of the limb. The enrichment of Ca in the garnet from the hinge and its depletion in the garnet from the limb at XMn = 0.008–0.009 possibly suggest a transfer of Ca from the limb to the hinge and its subsequent fixation in the crystallizing garnet. Our microstructural observations have documented that a change in the stress field occurred after a relative rotation of 270°, along with a change in the nature of inclusion pattern formation. Quantitative compositional data show that this transition occurred precisely at XMn = 0.008–0.009, strongly suggesting that the modification of the stress field led to a change in rock chemistry in the garnet from the hinge, and to the cessation of growth of the garnet from the limb.

CRYSTALLOGRAPHIC ORIENTATION

Several recent studies have shown that crystallographic orientations measured by EBSD provide valuable data to constrain nucleation and growth processes of garnet porphyroblasts (Spear & Daniel, 2001; Spiess *et al.*, 2001, 2007; Hirsch *et al.*, 2003; Storey & Prior, 2005; Robyr *et al.*, 2007; Bestmann *et al.*, 2008; Whitney *et al.*, 2008). Under the assumption of continuous incorporation of atoms onto the pre-existing garnet structure during growth, a single crystallographic orientation would be expected for the entire spiral. Likewise, because individual snowball garnet nucleated independently of one another, a random distribution of crystallographic orientations might be expected for the entire garnet population.

Previous analyses of crystallographic orientation performed on snowball garnet from the fold hinge (Robyr *et al.*, 2007), however, revealed that the garnet spirals are composed of several crystallographic domains. Whereas the core region is characterized by a single crystallographic orientation, the arm terminations are made of smaller box-shaped domains having distinct crystallographic orientations (Fig. 10a,c). Comparison between EBSD and chemical data showed that most of the external domains are centred on secondary Mn maxima (Robyr *et al.*, 2007) and that the boundaries between adjacent domains are straight and coincide with low-Mn interfaces (Fig. 10b). These features strongly suggest that the growth of the external domains started from individual nucleation sites and resulted in converging crystallization fronts that

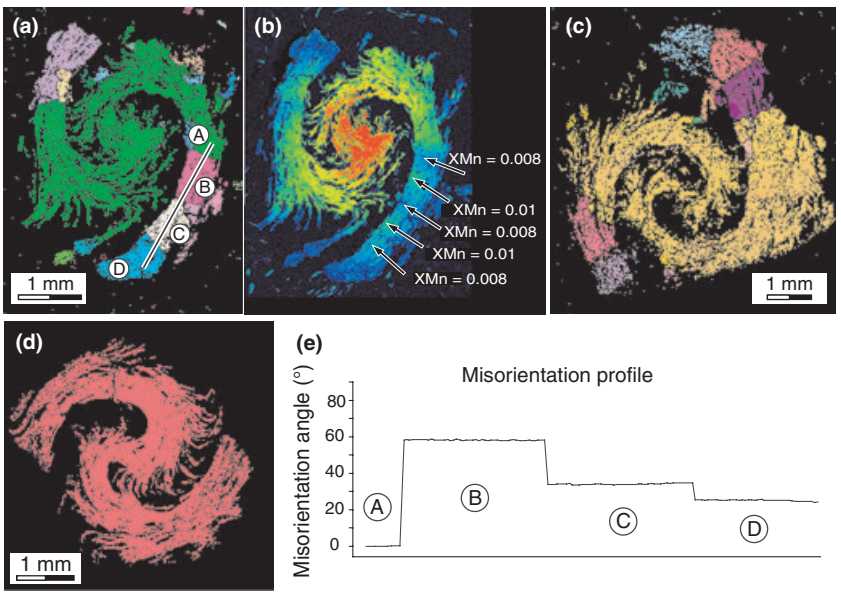

Fig. 10. EBSD crystallographic-orientation maps for the samples collected in the hinge (a,c) and in the limb (d). (b) WDS X-ray map of Mn for the sample shown in (a), with concentration decreasing from red to blue. (e) Misorientation profile for the garnet shown in (a).

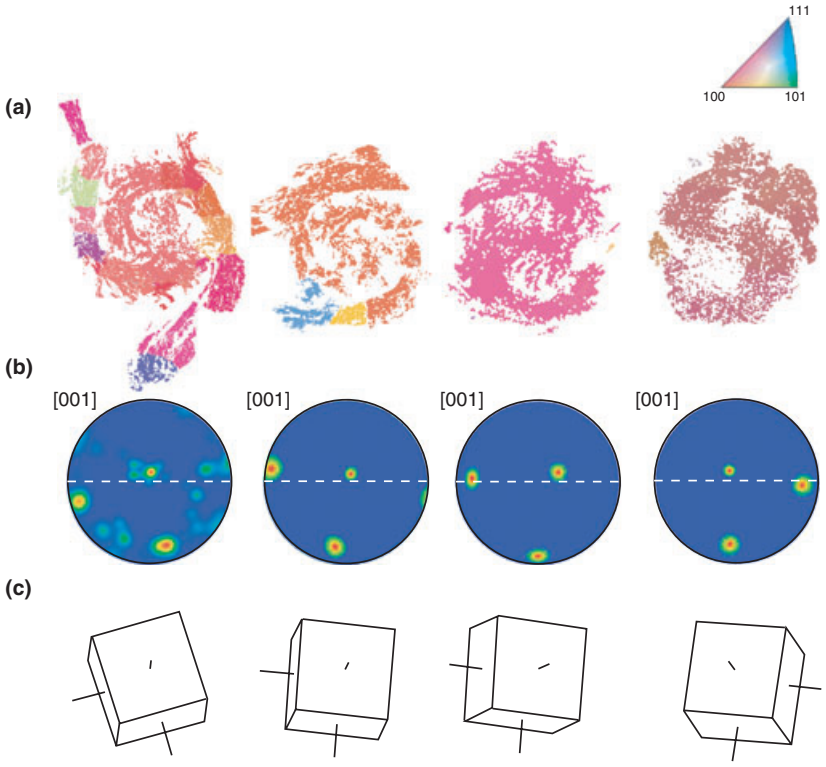

Fig. 11. (a) EBSD inverse pole figure maps showing the crystallographic axes falling parallel to the garnet symmetry axis (page normal). (b) Pole figures of garnet [001] for the central domain of the porphyroblasts shown in (a). Pole figures are represented on upper hemisphere equal-area projections. The foliation trace, recorded as inclusion trails in the core region, is indicated by a dashed line. (c) Garnet unit cells illustrating the crystallographic orientation of garnet [001] in the central domain.

abutted against each other during the final stage of the garnet growth history. The magnitude of the crystallographic misorientation between the different domains, typically a few tens of degrees (Fig. 10d), completely rules out the possibility that the domains are subgrains resulting from plastic deformation. In addition, the perfect continuity of the inclusion trails across the boundaries precludes postcrystallization rupture of the spiral arms as a potential mechanism accounting for the formation of the different crystallographic domains. However, as the external domains are thought to have nucleated and grown during flexural folding (D3), we cannot exclude that a readjustment of the garnet nuclei-bearing phyllosilicate stacks located in the prolongation of the spiral core might have contributed to the misorientation observed between the external domains and between the external domains and the spiral core.

In the garnet from the hinge, the core region never extends beyond the first 270° of the spiral, whereas the external domains comprise the last 90° of the spiral. In the limb, the 270°-rotated garnet show only one crystallographic orientation for the entire spiral (Fig. 10e), i.e. box-shaped domains having distinct crystallographic orientations are never observed for those grains. The EBSD results are therefore consistent with the microstructural and geochemical observations. In the hinge, the modification of the stress field and the change in rock chemistry that occurred at XMn = 0.008–0.009 after 270° of rotation was also accompanied by a change of growth style leading to the formation of external domains having different crystallographic orientations. In the limb, the cessation of growth after a 270° rotation explains the absence of external domains.

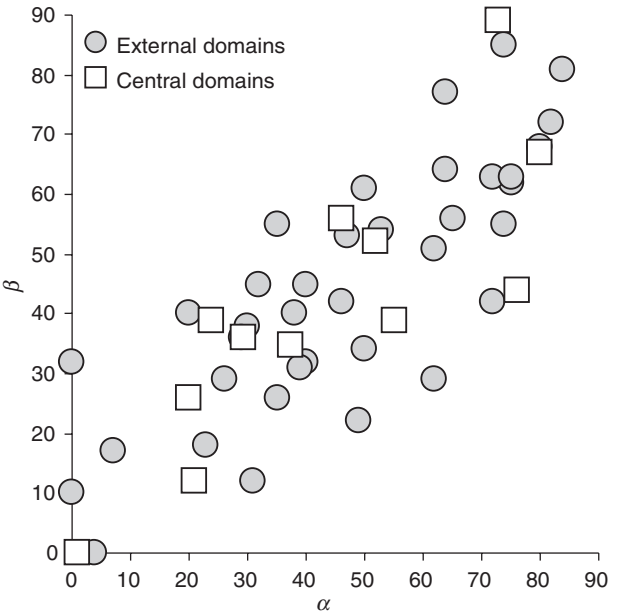

Fig. 12. Diagram showing the correlation between the orientation of the internal foliation and the orientation of the garnet [001] axis. α = misorientation angle between the foliation and the vertical edge of the thin section. β = misorientation angle between garnet [001] and the vertical edge of the thin section.

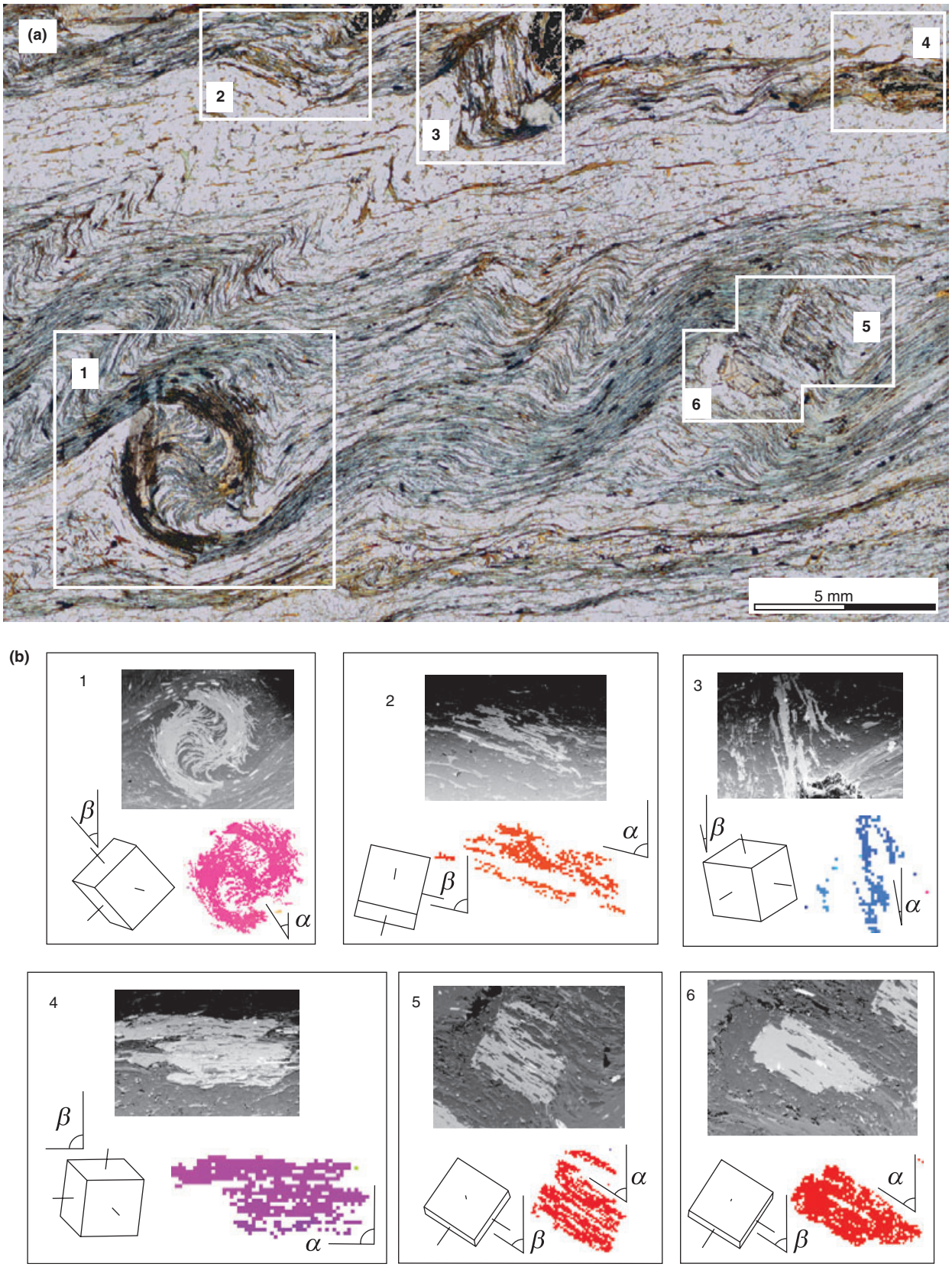

Fig. 13. (a) Photomicrograph of a thin section from the fold limb. (b) BSE and EBSD data for the garnet framed in (a) showing the strong correlation between α and β (legend as in Fig. 12).

RELATIONSHIPS BETWEEN CRYSTALLOGRAPHIC ORIENTATION AND INTERNAL FOLIATION

Electron backscattered diffraction maps of snowball garnet from both the hinge and the limb highlight a correlation between the crystallographic orientation and the orientation of the symmetry axis. Sections perpendicular to the symmetry axis show that garnet $<001>$ has one axis oriented (sub-)parallel to the symmetry axis and one axis normal to it oriented (sub-) parallel to the internal foliation (recorded as inclusion trails in the core of the spiral) (Fig. 11). The orientation of the crystallographic axes with respect to the internal foliation was measured for 50 distinct domains belonging to 10 different snowball garnet (Fig. 12). These data reveal that the correlation observed in the core region between the crystallographic orientation and the internal foliation is valid for the external domains of the arm terminations as well. In addition, EBSD was also performed on several garnet from the fold limb (Fig. 13) having either usual helicitic inclusion trails or straight internal foliation. Again a strong correlation was noted between the orientation of the internal foliation and the garnet [001] axis, whatever the geometry of the inclusion trails. As a consequence, the systematic correlation between the crystallographic orientation of garnet and the orientation of the internal foliation indicates that the crystallographic orientation of the snowball garnet is not random.

Previous studies (Frondel, 1940; Powell, 1966) highlighted some systematic relationships in crystallographic orientation between garnet and mica. Analogous observations were reported recently by Spiess *et al.* (2007). These authors showed that the pseudo-hexagonal oxygen ring structure of the biotite (001) basal plane could provide a template for the oxygen atoms located on garnet {110}. Our EBSD data reveal that one [001] axis in snowball garnet is parallel to the symmetry axis *and* another [001] axis is parallel to the internal foliation (recorded as inclusion trails in the garnet core). An epitaxial growth of garnet {110} onto the basal (001) mica plane, as reported in previous studies, would result in only one garnet [001] axis lying within the (001) mica plane. To match our observations, a garnet nucleating in this orientation would have to be rotated early in its development in order to bring a second [001] axis into the foliation plane and the snowball garnet symmetry axis normal to the shear sense.

In contrast to the observations of Spiess *et al.* (2007), our data suggest epitaxial growth of garnet {001}, not {110} on the (001) mica plane. This orientation would require, after nucleation, a single rotation of the newly formed garnet around an axis normal to the foliation in order to bring simultaneously one [001] axis parallel to the shear sense and another [001] axis parallel to the snowball garnet symmetry axis. Alternatively, one could imagine full crystallographic control of the entire set of garnet $<001>$ directions by precursor phyllosilicates. That hypothesis, however, would require a preferred orientation for phyllosilicate [010] within the foliation plane *and* a crystallographic control fixing this axis parallel to garnet [001]. The very specific circumstances necessary for this latter scenario, added to the fact that the hypothesis is not supported by the crystallographic arrangement of atoms on garnet {001} and the mica (001) plane, make it unlikely.

Finally, it must be stressed that full understanding of epitaxial growth of garnet on phyllosilicates can be achieved only if the complete crystallographic orientation of phyllosilicates within the foliation plane is known at the location where garnet has nucleated. These conditions are not fulfilled in this study.

CONCLUSIONS

The growth of the snowball garnet from the Lukmanier Pass area was investigated based on microstructural, geochemical and crystallographic-orientation analyses coupled with regional tectonics. The most significant results are summarized as follows.

During D2, garnet started to nucleate, possibly epitaxially and grew in phyllosilicate-rich layers of the dominant S2 foliation. At that time, all garnet shared the same history, characterized by simultaneous growth and rotation under non-coaxial flow. The smooth spiral-shaped inclusion trails, the concentric geochemical record and the preservation of a single crystallographic orientation indicate that this phase of garnet growth was regular and non-chaotic, even if crystallization across bridges was sometimes preferred to the standard crystallization path along the spiral curvature. At the end of D2, the garnet had acquired a 270° spiral shape. During D3, the flexural folding that affected the entire Lukmanier Pass area initiated a radical change in the development of the snowball garnet, associated with a transfer of chemical elements from the limb to the hinge. Whereas the garnet located in the fold limb did not grow further, that in the hinge continued to grow, overprinting the crenulated S2 foliation under a non-rotational flow regime. Garnet started to grow from individual nucleation sites within the phyllosilicate stacks, as documented by secondary Mn maxima centred in box-shaped domains having distinct crystallographic orientations. At the end of D3, the garnet from the hinge reached their final shape, with an apparent rotation of 360°.

Our results suggest that as long as growth is accompanied by rotation, the primary core orientation is preserved, but once the rotation stops the crystallographic orientation is prone to change. In addition, it has been shown that the crystallographic orientations of the different garnet domains are not random; instead, a relation exists among the symmetry axis, the internal foliation and crystallographic orientation. This feature is interpreted as evidence for a crystallographic control of phyllosilicates onto the nucleating garnet.

Finally, this study illustrates the power of combining microstructural observations with geochemical and crystallographic-orientation analyses. In particular, EBSD is shown to be a very effective tool for highlighting changes in growth regime within snowball garnet and potentially also for helping to distinguish between rotational and non-rotational models. Further efforts, applying a similar approach in other locales, should be expected to advance the debate over rotational *v*. non-rotational porphyroblast growth beyond the impasse reached by application of microstructural analysis alone.

ACKNOWLEDGEMENTS

This study was supported by the Swiss National Science Foundation (PA002-113173) and by the Jackson School of Geosciences (University of Texas at Austin). The HRXCT facility at the University of Texas is supported by NSF grant EAR-0646848. Jane Selverstone and Richard Spiess provided thoughtful reviews that were a great help in clarifying the paper. Special thanks to all the people of the Jackson School of Geosciences who contributed to make the postdoctoral stay of the first author so pleasant.

REFERENCES

Aerden, D. G. A. M., 1995. Porphyroblast non-rotation during crustal extension in the Variscan Lys-Caillaouas Massif, Pyrenees. *Journal of Structural Geology*, **17,** 709–725.

Bell, T. H., 1985. Deformation partitioning and porphyroblast rotation in metamorphic rocks: a radical re-interpretation. *Journal of Metamorphic Geology*, 109–118.

Bell, T. H. & Hickey, K. A., 1999. Complex microstructures preserved in rocks with a simple matrix: significance for deformation and metamorphic process. *Journal of Metamorphic Geology*, **17,** 521–536.

Bell, T. H. & Johnson, S. E., 1989. Porphyroblast inclusion trails: the key to orogenesis. *Journal of Metamorphic Geology*, **7,** 279–310.

Bell, T. H. & Rubenach, M. J., 1983. Sequential porphyroblast growth and crenulation cleavage development during progressive deformation. *Tectonophysics*, **92,** 171–194.

Bell, T. H., Johnson, S. E., Davis, B., Forde, A., Hayward, N. & Witkins, C., 1992. Porphyroblast inclusion-trail orientation data; eppure non son girate! *Journal of Metamorphic Geology*, **10,** 295–307.

Bestmann, M., Habler, G., Heidelbach, F. & Thöni, M., 2008. Dynamic recrystallization of garnet and related diffusion processes. *Journal of Structural Geology*, **30,** 777–790.

Busa, M. D. & Gray, N. H., 1992. Rotated staurolite porphyroblasts in the Littleton Schist at Bolton, Connecticut, USA. *Journal of Metamorphic Geology*, **10,** 627–636.

Carlson, W. D., 1989. The significance of intergranular diffusion to the mechanisms and kinetics of porphyroblast crystallization. *Contributions to Mineralogy and Petrology*, **103,** 1–24.

Carlson, W. D., 1991. Competitive diffusion-controlled growth of porphyroblasts. *Mineralogical Magazine*, **55,** 317–330.

Carlson, W. D. & Denison, C., 1992. Mechanisms of porphyroblast crystallization: results from high-resolution computed X-ray tomography. *Science*, **257,** 1236–1239.

Carlson, W. D., Denison, C. & Ketcham, R. A., 1995. Controls on the nucleation and growth of porphyroblasts: kinetics from natural textures and numerical models. *Geological Journal*, **30,** 207–225.

Chadwick, B., 1968. Deformation and metamorphism in the Lukmanier region, Central Switzerland. *Geological Society of America Bulletin*, **79,** 1123–1149.

Chernoff, C. & Carlson, W. D., 1997. Disequilibrium for Ca during growth of pelitic garnet. *Journal of Metamorphic Geology*, **15,** 421–438.

Chernoff, C. & Carlson, W. D., 1999. Trace element zoning as a record of chemical disequilibrium during garnet growth. *Geology*, **27,** 555–558.

Daniel, C. G. & Spear, F. S., 1999. The clustered nucleation and growth processes of garnet in regional metamorphic rocks from North-west Connecticut, USA. *Journal of Metamorphic Geology*, **17,** 503–520.

Denison, C., Carlson, W. D. & Ketcham, R. A., 1997. Three dimensional quantitative textural analysis of metamorphic rocks using high-resolution computed X-ray tomography. Part I. Methods and techniques. *Journal of Metamorphic Geology*, **15,** 29–44.

Forde, A. & Bell, T. H., 1993. The rotation of garnet porphyroblasts around a single fold, Lukmanier Pass, Central Alps: discussion and reply. *Journal of Structural Geology*, **15,** 1365–1372.

Fox, J. S., 1975. Three-dimensional isograds from the Lukmanier Pass, Switzerland, and their tectonic significance. *Geological Magazine*, **112,** 547–564.

Frondel, C., 1940. Oriented inclusions of staurolite, zircon and garnet in muscovite. Skating crystals and their significance. *American Mineralogist*, **25,** 69–87.

Gray, N. H. & Busa, M. D., 1994. The three-dimensional geometry of simulated porphyroblasts inclusion trails: inert-marker, viscous-flow models. *Journal of Metamorphic Geology*, **12,** 575–587.

Hickey, K. A. & Bell, T. H., 1999. Behaviour of rigid objects during deformation and metamorphism: a test using schists from the Bolton syncline, Connecticut, USA. *Journal of Metamorphic Geology*, **17,** 21–228.

Hirsch, D. M., Prior, D. J. & Carlson, W. D., 2003. An overgrowth model to explain multiple, dispersed high-Mn regions in the cores of garnet porphyroblasts. *American Mineralogist*, **88,** 131–141.

Hollister, L. S., 1966. Garnet zoning: an interpretation based on the Rayleigh fractionation model. *Science*, **154,** 1647–1651.

Ikeda, T., Shimobayashi, N., Wallis, S. R. & Tsuchiyama, A., 2002. Crystallographic orientation, chemical composition and three-dimensional geometry of sigmoidal garnet; evidence for rotation. *Journal of Structural Geology*, **24,** 1633–1646.

Janots, E., Engi, M., Berger, A., Allaz, J., Schwarz, J. O. & Spandler, C., 2008. Prograde metamorphic sequence of REE minerals in pelitic rocks of the Central Alps: implications for allanite–monazite–xenotime phase relations from 250 to 610°C. *Journal of Metamorphic Geology*, **26,** 509–526.

Johnson, S. E., 1990. Lack of porphyroblast rotation in the Otago schists, New Zealand: implications for crenulation cleavage development, folding and deformation partitioning. *Journal of Metamorphic Geology*, **8,** 13–30.

Johnson, S. E., 1993. Testing models for the development of spiral-shaped inclusion trails in garnet porphyroblasts: to rotate or not to rotate, that is the question. *Journal of Metamorphic Geology*, **11,** 635–659.

Johnson, S. E. & Bell, T. H., 1996. How useful are "millipede" and other similar porphyroblast microstructures for determining synmetamorphic deformation histories? *Journal of Metamorphic Geology*, **14,** 15–28.

Kretz, R., 1973. Kinetics of the crystallization of garnet at two localities near Yellowknife. *The Canadian Mineralogist*, **12,** 1–20.

Kretz, R., 1974. Some models for the rate of crystallization of garnet in metamorphic rocks. *Lithos*, **7,** 123–131.

Kretz, R., 1993. A garnet population in Yellowknife Schist, Canada. *Journal of Metamorphic Geology*, **11,** 101–120.
Mancktelow, N. S., Arbaret, L. & Pennacchioni, G., 2002. Experimental observations on the effect of interface slip on rotation and stabilization of rigid particles in simple shear and comparison with natural mylonites. *Journal of Structural Geology*, **24,** 567–585.
Maxelon, M. & Mancktelow, N. S., 2005. Three-dimensional geometry and tectonostratigraphy of the Pennine zone, Central Alps, Switzerland and northern Italy. *Earth-Science Reviews*, **71,** 171–227.
Meth, C. M. & Carlson, W. D., 2005. Diffusion-controlled synkinematic growth of garnet from a heterogeneous precursor at Passo del Sole, Switzerland. *The Canadian Mineralogist*, **43,** 157–182.
Passchier, C. W. & Trouw, R. A. J., 2005. *Microtectonics*. Springer Verlag, Berlin, 289 p.
Passchier, C. W., Trouw, R. A. J., Zwart, H. J. & Vissers, R. L. M., 1992. Porphyroblast rotation; eppur si muove? *Journal of Metamorphic Geology*, **10,** 283–294.
Powell, D., 1966. On the preferred crystallographic orientation of garnet in some metamorphic rocks. *Mineralogical Magazine*, **35,** 1094–1109.
Rahn, M. K., Steinmann, M. & Frey, M., 2002. Chloritoid composition and formation in the Central Alps: a comparison between Penninic and Helvetic occurrences. *Schweizerische Mineralogische und Petrographische Mitteilungen*, **82,** 409–426.
Ramsay, J. G., 1962. The geometry and mechanics of formation of 'similar' type folds. *Journal of Geology*, **70,** 309–327.
Robyr, M., Vonlanthen, P., Baumgartner, L. P. & Grobety, B., 2007. Growth mechanism of snowball garnets from the Lukmanier Pass area (Central Alps, Switzerland): a combined μCT/EMPA/EBSD study. *Terra Nova*, **19,** 240–244.
Rosenfeld, J. L., 1970. Rotated garnets in metamorphic rocks. *Geological Society of America Special Paper*, **129,** 105.
Schmid, D. W. & Podladchikov, Y. Y., 2004. Are isolated stable rigid clasts in shear zones equivalent to voids? *Tectonophysics*, **384,** 233–242.
Schoneveld, C., 1977. A study of some typical inclusion patterns in strongly paracrystalline-rotated garnets. *Tectonophysics*, **39,** 453–471.
Spear, F. S., 1993. *Metamorphic Phase Equilibria and Pressure-Temperature-Time Paths*. Mineralogical Society of America, Washington, D.C.
Spear, F. S. & Daniel, C. G., 1998. 3-dimensional imaging of garnet porphyroblast sizes and chemical zoning; nucleation and growth history in the garnet zone. *Geological Materials Research*, **1,** 1–43.
Spear, F. S. & Daniel, C. G., 2001. Diffusion control of garnet growth, Harpswell Neck, Maine, USA. *Journal of Metamorphic Geology*, **19,** 179–195.
Spiess, R., Peruzzo, L., Prior, D. J. & Wheeler, J., 2001. Development of garnet porphyroblasts by multiple nucleation, coalescence and boundary misorientation-driven rotations. *Journal of Metamorphic Geology*, **19,** 269–290.
Spiess, R., Groppo, C. & Compagnoni, R., 2007. When epitaxy controls garnet growth. *Journal of Metamorphic Geology*, **25,** 439–450.
Spry, A., 1963. The origin and significance of snowball structure in garnet. *Journal of Petrology*, **4,** 211–222.
Stallard, A., 2003. Comment on "Crystallographic orientation, chemical composition and three-dimensional geometry of sigmoidal garnet: evidence for rotation" by T. Ikeda, N. Shimobayashi, S. Wallis & A. Tsuchiyama. *Journal of Structural Geology*, **25,** 1337–1339.
Stallard, A., Ikei, H. & Masuda, T., 2002. Quicktime movies of 3D spiral inclusion trails development. In: *Visualization, Teaching and Learning in Structural Geology* (ed. Bobyarchick, A.). *Journal of the Virtual Explorer*, **9,** 1–14.
Storey, C. D. & Prior, D. J., 2005. Plastic deformation and recrystallization of garnet: a mechanism to facilitate diffusion creep. *Journal of Petrology*, **46,** 2593–2613.
Thakur, V. C., 1973. Events in Alpine deformation and metamorphism in the N. Apline zone and S. Gotthard Massif regions. *Geologische Rundschau*, **62,** 549–563.
Todd, C. S. & Engi, M., 1997. Metamorphic field gradients in the Central Alps. *Journal of Metamorphic Geology*, **15,** 513–530.
Vernon, R. H., Paterson, S. R. & Foster, D., 1993. Growth and deformation of porphyroblasts in the Foothill terrane, central Sierra Nevada, California: negotiating a microstructural minefield. *Journal of Metamorphic Geology*, **11,** 203–222.
Visser, P. & Mancktelow, N. S., 1992. The rotation of garnet porphyroblasts around a single fold, Lukmanier Pass, Central Alps. *Journal of Structural Geology*, **14,** 1193–1202.
Whitney, D. L., Goergen, E. T., Ketcham, R. A. & Kunze, K., 2008. Formation of garnet polycrystals during metamorphic crystallization. *Journal of Metamorphic Geology*, **26,** 365–383.
Williams, P. F. & Jiang, D., 1999. Rotating garnet. *Journal of Metamorphic Geology*, **17,** 367–378.

Received 11 July 2008; revision accepted 10 May 2009.